Nuclear Physics A505 (1989) 835-848
North-Holland, Amsterdam

# ELECTROMAGNETIC PHYSICS AT RELATIVISTIC HEAVY ION COLLIDERS, FOR BETTER AND FOR WORSE

G. BAUR and C.A. BERTULANI[1]

*Institut für Kernphysik, Kernforschungsanlage Jülich GmbH, Postfach 19 13, D-5170 Jülich, Fed. Rep. Germany*

Received 20 June 1989
(Revised 25 July 1989)

**Abstract:** Relativistic heavy-ion colliders in the 100 GeV/$A$ and several TeV/$A$ region are planned and considered in Brookhaven and at CERN. Cross sections for electromagnetic processes in distant collisions are large; they are studied in view of their practical importance in the collider design (limitations on luminosity half-life due to electromagnetic fragmentation process and $e^+e^-$ pair production with $e^-$ capture) as well as for their potential for basic physics (like Higgs boson production in $\gamma\gamma$ collisions). We especially consider giant dipole excitation, lepton pair creation and $\gamma\gamma$ physics.

## 1. Introduction

Relativistic heavy-ion (RHI) colliders are planned and considered in Brookhaven (RHIC) [1]) and at CERN (LHC) [2]). The main interest in this kind of collisions has been the study of a new phase of matter (quark–gluon plasma) in central nuclear collisions. It is the purpose of this paper to study the effects of the electromagnetic processes which occur in even very distant collisions with no nuclear contact. These effects are of very long range and can be very strong for high-$Z$ projectiles. This is of twofold importance for RHI colliders:

(i) due to fragmentation processes, induced by the electromagnetic excitation, and to lepton (mainly electron) pair creation processes the ion beam looses particles, or energy, or changes their charge state ($e^+e^-$ pair creation and $e^-$ capture). This leads to a decrease of luminosity with time, and it should be taken into account appropriately in the design parameters. Since in general the response of nuclei to the electromagnetic interaction is known quite well, safe predictions are possible.

(ii) since the RHI's can be considered as a strong source of hard equivalent photons, a new way to study $\gamma\gamma$ physics could open up. The essential advantage is a factor $Z^4$ (in symmetric collisions) in the cross section, as compared to $e^+e^-$ colliders. However, strong interaction and other background problems have to be seriously studied.

[1] Permanent address: Instituto de Fisica, Universidade Federal do Rio de Janeiro, 21945 Rio de Janeiro, RJ, Brazil.

The interaction of the very sudden electromagnetic pulse due to the passage of one nucleus leads to the electromagnetic excitation of the other one. This will be studied in sect. 2. Especially large is the effect of the excitation of the giant dipole resonance, since it decays mainly by particle emission. This leads to a beam loss. In sect. 3 we study the effects of lepton pair production. The production of $e^+e^-$ pairs is most important due to their low mass. When the electron is produced in a bound atomic state, the charge of the ion is changed, resulting in an immediate beam loss. We calculate the energy loss spectra; this will be important for considerations of beam stability [2]). The pair production mechanism also contributes to the stopping power of cosmic-ray nuclei. Being linear in $\gamma$ (the Lorentz factor in the centre-of-mass system), it will outweigh for high enough $\gamma$, the contribution due to electronic collisions as given by the Bethe–Bloch formula. In sect. 4 we investigate the use of RHI colliders for $\gamma\gamma$ reactions which might be investigated. Our conclusions are given in sect. 5.

Fairly recent reviews on electromagnetic processes in RHI collisions are given in refs. [3,4]), a preliminary account of part of the present work is given in ref. [5]).

In our numerical examples we choose the systems U + U at $\gamma = 100$ (corresponding to RHIC plans [1]) and the systems Pb + Pb, La + La and Sr + Sr at $E/A = 4000$ GeV/$A$ (being considered for LHC [2]). Since the cross sections vary essentially logarithmically with $\gamma$, and since there are rather simple and accurate scaling laws with respect to $Z$ and $A$, we think that the presently studied examples will give an accurate and detailed picture of what is to be expected.

## 2. Electromagnetic excitation and fragmentation of nuclei

The cross sections for Coulomb, or electromagnetic, excitation of nuclei can be written as a product of a kinematical factor and the photonuclear cross section, i.e., the cross sections induced by a real photon. The kinematical factors are interpreted as the number of equivalent photons incident on the nucleus [see refs. [3,4]) and further references given there]. Since the Lorentz factors $\gamma_p$, as viewed in a system where one of the nuclei is at rest, are very high (they are given by

$$\gamma_p = 2\gamma^2 - 1 , \tag{2.1}$$

where $\gamma$ is the Lorentz factor in the c.m. system), the corresponding equivalent photon spectrum is very hard, i.e., it contains a large amount of highly energetic photons.

The largest part of the photoabsorption cross section corresponds to the excitation of the giant dipole resonance (GDR) in the nuclei. Such excited states decay mainly by particle emission, or by fission, in the case of very heavy nuclei, contributing largely to the total fragmentation cross section in RHI collisions [6,7]). Further effects (at the 10% level), in the energy range of some tens of MeV, are the excitation of collective E2 strength and the quasi-deuteron effect. Experimental investigations at the highest presently available energies (200 GeV/$A$) were made by various groups with target [6]) and projectile [7]) fragmentation at the CERN heavy-ion beam. They are in essential agreement with the theoretical calculations [3,4]). In order to obtain an accurate overview we can assume that the giant dipole resonance exhausts the Thomas–Reiche–Kuhn sum rule and is located at $E_{\mathrm{GDR}} = 80A^{-1/3}$ MeV, where $A$ is the mass number. The total cross section for symmetric systems is [3])

$$\sigma_{\mathrm{GDR}} = 3.42 \frac{NZ^3}{A^{2/3}} \ln \gamma_{\mathrm{p}}\ (\mu\mathrm{b})\,. \tag{2.2}$$

The corresponding numbers for the typical examples are collected table 1. The one-photon exchange process with the logarithmic rise with $\gamma_{\mathrm{p}}$ is the dominant effect. Multiphoton exchange processes, like the excitation of multiphonon giant dipole modes [8]) or surface vibrations coupled to giant resonance states [9]) will lead to a constant value for $\gamma_{\mathrm{p}} \to \infty$ (<1 b). Therefore, as compared to the first-order process, they are not so important for the present considerations of beam loss.

There are also sizeable contributions due to electromagnetic excitation in the region of nucleon (especially $\Delta$) resonances. In ref. [3]) the experimentally known $\gamma$N (nucleon) total cross sections was folded with the equivalent photon spectrum. In order to take shadowing into account [10]), one can multiply the elementary $\gamma$N cross section by $A^{\alpha}$ with $\alpha = 0.6$. After that one obtains a simple scaling law (see eq. (3.3.3) of ref. [3])) given by

$$\sigma_{\mathrm{prod}}(E_{\gamma} < 2\ \mathrm{GeV}) \simeq 10^{-2} A^{\alpha} Z^2 \ln\left(\tfrac{1}{10}\gamma_{\mathrm{p}}\right)\ (\mathrm{mb})\,, \tag{2.3}$$

where the factor $\frac{1}{10}$ in the logarithm comes from the factor $\hbar c\gamma_{\mathrm{p}}/\hbar\omega R$, which appears in the equivalent photon spectrum for $\gamma_{\mathrm{p}} \gg 1$, where $R$ is the sum of the nuclear radii. For $\hbar\omega > 140$ MeV (threshold for $\pi$-production) the first and largest peak occurs at $\hbar\omega \sim 300$ MeV, corresponding to the $\Delta$-excitation. Taking $\hbar\omega$ at this peak the factor $\frac{1}{10}\gamma_{\mathrm{p}}$ in (2.3) is obtained. With this law we obtain the numbers collected in table 1. Although smaller than the values found or GDR excitation they are a non-negligible source of beam loss. It is worth mentioning that experiments with 60 and 200 GeV/$A$ heavy-ion beams at CERN [7,11]) have verified this contribution ("electromagnetic spallation") and the formula above may be considered as a safe prediction of (electromagnetic) hadron production in RHI collisions.

Some ambiguities will remain in the theoretical predictions of the contributions from equivalent photon energies above the nucleon resonance region, i.e., for $E_{\gamma} > 2$ GeV. At least, this is the case for the LHC energies, which correspond to $\gamma_{\mathrm{p}} = 3.6 \times 10^7$. This leads to equivalent photon energies up to $E_{\gamma}^{\max} = \gamma_{\mathrm{p}} \hbar c/R \simeq$ 500 TeV, which is a hitherto experimentally unexplored ($\gamma$N) energy region. If we assume a constant value of $\sigma_{\gamma\mathrm{N}} = 100\ \mu$b, we find

$$\sigma_{\mathrm{prod}}(E_{\gamma} > 2\ \mathrm{GeV}) \simeq 0.46 A^{\alpha} Z^2 \ln^2\left(\tfrac{1}{2}E_{\gamma}^{\max}\right)\ (\mu\mathrm{b}) \tag{2.4}$$

with $E_{\gamma}^{\max}$ given in GeV. Using this formula we obtain the numbers given in table 1 (for RHIC, $E_{\gamma}^{\max} \simeq 300$ GeV). However, it must be borne in mind that this

TABLE 1

Cross section for electromagnetic processes in RHI colliders (in barns)

| System | GDR | Nucleon resonance region, $E_\gamma < 2$ GeV | $E_\gamma > 2$ GeV (assuming $\sigma = \text{const} = 100\ \mu$b) | $e^+e^-$ pairs (free) | $Z+Z \to (Z+e^-) + e^+ + Z$ |
|---|---|---|---|---|---|
| U+U RHIC | 100 | 17 | 2.6 | 77 000 | 80 |
| Sr+Sr LHC | 8.3 | 3.2 | 0.24 | 13 000 | 2 |
| La+La LHC | 34 | 9.5 | 0.33 | 67 000 | 19.3 |
| Pb+Pb LHC | 118 | 25 | 19 | 290 000 | 106 |

Except for the production of free $e^+e^-$ pairs, the values refer to one nucleus. At RHIC, $\gamma = 100$, and at LHC, $\gamma = 4000$, is assumed.

extrapolation of an energy-independent total $\gamma$N cross section is quite uncertain. For 2 GeV up to about 200 GeV (the highest measured energy [12])) the cross section can be approximated by $\sigma_{\gamma N} = 100\ \mu$b for our present purposes, so that the values given in table 1 for the RHIC case are probably a good estimate. On the other hand, one could use this extremely hard part of the equivalent photon spectrum in order to measure $\gamma$N cross sections in this hitherto unaccessible energy range.

## 3. Lepton pair production and luminosity loss

Lepton pair production in RHI collisions due to the $\gamma\gamma$ mechanism is copious and has been studied by many authors [3,13,14]). This mechanism dominates over the bremsstrahlung pair-production mechanism due to the large mass of the ions [15,16]). The cross section for lepton pair production in RHI colliders is given by

$$\sigma_{\ell^+\ell^-} = \frac{28}{27\pi} (Z_1 Z_2 \alpha r_\ell)^2 \ln^3 (\tfrac{1}{2}\gamma_p) , \qquad (3.1)$$

where $r_\ell = e^2/m_\ell^2$ with $m_\ell$ equal to the lepton mass ($\ell =$ e, $\mu$ or $\tau$). This formula [16]) is a good approximation for $e^+e^-$ production if $\gamma_p \gg 1$. It also describes well $\mu^+\mu^-$ and $\tau^+\tau^-$ production if $\gamma_p \gg 20$ and $\gamma_p \gg 300$, respectively [14]). Both conditions are satisfied at RHIC, as well as at LHC. Cross sections for the production of free $e^+e^-$ pairs is huge, as seen in table 1. From (3.1) one sees that the production of free $\mu^+\mu^-$ (or $\tau^+\tau^-$) pairs can be obtained by scaling with the mass factor $(m_e/m_\ell)^2$ ($\ell = \mu$ or $\tau$). For example, the $\mu^+\mu^-$ pair production cross section in Pb-Pb collisions with $\gamma_p = 3.6 \times 10^7$ is found to be 6.9 barns.

A direct source of beam loss will be the capture process [3,14])

$$Z + Z \to (Z + e^-)_{K,L,\ldots} + e^+ + Z \qquad (3.2)$$

which changes the charge state of the ions. For $Z\alpha \ll 1$, the cross sections for this process were first calculated in ref. [3]) and is given by

$$\sigma_{e^+e^-} \simeq 12.6 Z^8 \alpha^6 r_e^2 \frac{1}{e^{2\pi Z\alpha}-1} \ln(\gamma_p/15.5) , \tag{3.3}$$

where capture in all atomic shells are included. The capture is mainly proceeded into the K-shell. Capture into other orbits contributes about 20% to the cross section. The formula (3.3) is obtained using lepton wave functions which are valid for $Z\alpha \ll 1$. Thus, for very precise values for the high-$Z$ cases, the use of more accurate lepton wave functions will become necessary [17]).

The loss of particles $dN/dt$ in the ring per unit time is given by

$$\frac{dN}{dt} = -kL\sigma , \tag{3.4}$$

where $k$ is the number of intersections, $L$ the luminosity and $\sigma$ the total cross section for loss processes. Let us take the number from the CERN plans as an example. We assume $^{208}Pb + ^{208}Pb$, $L = 10^{28}\ cm^{-2}\,s^{-1}$, and $k = 3$, with a total capture cross section of 100 b (from the numbers given in table 1 we would surely underestimate the total loss cross section somewhat). We obtain $dN/dt = -3 \times 10^6\ s^{-1}$. The decay rate of the beam intensity is given by

$$\lambda = -\frac{1}{N}\frac{dN}{dt} = \frac{kL\sigma}{nb} , \tag{3.5}$$

where $b$ is the number of bunches and $n$ is the number of particles per bunch ($N = nb$). The luminosity is proportional to the square of the number of particles, and therefore the luminosity decays like

$$L = L_0 e^{-2\lambda t} , \tag{3.6}$$

where $L_0$ is the luminosity for $t = 0$. With the numbers for the CERN plans, $n = 1.6 \times 10^8$, $b = 643$, one obtains a luminosity decay constant of $2\lambda = (4h)^{-1}$. This is a strong limitation when one wants to run the beam for a period of 10 h[2]), only intrabeam scattering seems to pose more stringent limits on beam lifetime [2]).

The cross section for relativistic Coulomb fragmentation is somewhat larger than that of atomic capture. They also pose stringent beam losses. For the CERN plans the decay constant for Coulomb fragmentation is of the same order of the contribution due to $e^-$ capture. This gives a total decay constant of $2\lambda = (2h)^{-1}$.

Although the production of free $e^+e^-$ pairs does not lead to a direct loss of particles from the beam, a careful investigation of the effects of the energy loss on the beam behaviour is necessary. The basic quantity which one has to know is the differential energy loss spectrum (and the moments associated with it). The transverse momenta are very small in these peripheral processes, so we only deal here with the longitudinal components.

The differential energy loss spectrum $d\sigma/d\omega_1$ can be obtained quite simply and accurately by the following method (see fig. 1). Nucleus 1, travelling in the $+z$-direction emits an equivalent photon of energy $\omega_1$ (in the collider or lab system). This corresponds to the energy loss of ion 1. The equivalent photon interacts with nucleus 2 giving rise to $e^+e^-$ production. Using the Bethe-Heitler cross section (for an unscreened nucleus) and the equivalent photon spectrum relevant for pair-production we obtain

$$\frac{d\sigma}{d\omega_1}=\frac{2}{\pi}Z^2\alpha\frac{1}{\omega_1}\ln\left(\frac{\gamma m_e}{\omega_1}\right)\sigma_{\gamma Z\to e^+e^-Z}(\omega_{rel.})\,. \tag{3.7a}$$

The photon frequency $\omega_{rel.}$ as viewed from the system of nucleus 2 is given by

$$\omega_{rel.}=\frac{\omega_1}{\gamma(1-v)}\simeq 2\gamma\omega_1\,. \tag{3.7b}$$

The Bethe-Heitler cross section (for an unscreened nucleus, as is appropriate in the case of a collider) is given by [18])

$$\sigma_{\gamma Z\to e^+e^-Z}=\tfrac{28}{9}Z^2\alpha r_e^2\left[\ln\left(\frac{2\omega_{rel.}}{m_e}\right)-\tfrac{109}{42}-f(Z)\right], \tag{3.7c}$$

where

$$f(Z)=(Z\alpha)^2\sum_{n=1}^{\infty}\frac{1}{n(n^2+Z^2\alpha^2)}\,. \tag{3.7d}$$

The differential cross section becomes

$$\frac{d\sigma}{d\omega_1}=\frac{56}{9\pi}(Z^2\alpha r_e)^2\left\{\ln^2\gamma-\ln^2\left(\frac{\omega_1}{m_e}\right)+\ln\left(\frac{\gamma m_e}{\omega_1}\right)[\ln 4-\tfrac{109}{42}-f(Z)]\right\}. \tag{3.8}$$

The average energy loss is found to be

$$\begin{aligned}\langle\omega\sigma\rangle_{e^+e^-}&\equiv 2\int_{2m}^{\gamma m}d\omega\,\omega\frac{d\sigma}{d\omega}\\&=\frac{112}{9\pi}(Z^2\alpha r_e)^2 m_e\gamma\{2\ln\gamma+\ln 4-\tfrac{109}{42}-f(Z)\}\,.\end{aligned} \tag{3.9}$$

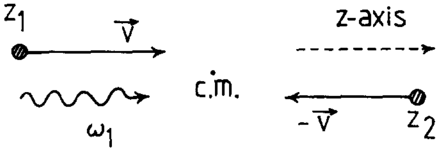


Fig. 1. Two heavy ions collide in the collider lab system. Ion 1 emits an equivalent (virtual) photon of energy $\omega_1$, this leads to an energy loss of $\omega_1$ of the ion 1 (in the lab system). This photon interacts with ion 2 and produces the $e^+e^-$ pair in the Bethe-Heitler process.

The factor 2 in the definition of eq. (3.9) arises because an energy loss happens to both nuclei. In addition, it is of interest to know the second moment for beam stability considerations [2])

$$\langle\omega^2\sigma\rangle_{e^+e^-} \equiv 2\int_{2m}^{\gamma m} d\omega\,\omega^2\frac{d\sigma}{d\omega}$$

$$=\frac{28}{9\pi}(Z^2\alpha r_e)^2 m_e^2\gamma^2\{2\ln\gamma-\ln 4+\tfrac{109}{42}+f(Z)\}\,. \tag{3.10}$$

In a collider with $k$ crossing points the energy loss per unit time is

$$\left(\frac{dE}{dt}\right)_{e^+e^-}=kL\langle\omega\sigma\rangle_{e^+e^-}\,. \tag{3.11}$$

For the CERN collider with $k=3$, $\gamma=4000$, $L=10^{28}\ \mathrm{cm}^{-2}\,\mathrm{s}^{-1}$ and for $^{208}$Pb beams, one finds $dE/dt=7.6\times10^{11}$ MeV/s $=1.3\times10^{-2}$ W.

We can also calculate the energy loss due to bremsstrahlung using eq. (3.7a) and the classical Thomson cross section

$$\sigma_{\gamma Z\to\gamma Z}=\frac{8\pi}{3}\left(\frac{Z^2e^2}{Am_N}\right)^2, \tag{3.12}$$

which is a good approximation for the scattering of the equivalent photons by a point like nucleus with charge $Z$ and mass $Am_N$, where $m_N$ is the nucleon mass. When folded with the equivalent photon numbers, one obtains

$$\left(\frac{d\sigma}{d\omega_1}\right)_{\text{brem.}}=\tfrac{16}{3}Z^6\alpha^3\lambda_N^2\frac{1}{\omega_1}\ln\left(\frac{\gamma}{\omega_1 R}\right), \tag{3.13}$$

where $\lambda_N=1/m_N$ is the nucleon Compton wavelength, and $R$ is the sum of the two nuclear radii. The energy loss by bremsstrahlung will be

$$\langle\omega\sigma\rangle_{\text{brem.}}\equiv\int_0^{\omega_b/2\gamma} d\omega\,\omega\frac{d\sigma}{d\omega}\simeq\tfrac{8}{3}Z^6\alpha^3\lambda_N^2\frac{\omega_b}{\gamma}\ln\left(\frac{2\gamma^2}{\omega_b R}\right), \tag{3.14}$$

where $\omega_b$ is the maximum energy for which the Thomson cross section is still a reasonable approximation for elastic $\gamma$-nucleus scattering. We take $\omega_b=10$ MeV, where deviations due to the excitation of giant resonances come into play. The upper limit of the integral in (3.14) comes from the use of the relation (3.7b).

For the collider plans at CERN, with the same parameters as in the examples above, we find that $\langle\omega\sigma\rangle_{e^+e^-}/\langle\omega\sigma\rangle_{\text{brem.}}\simeq 4\times10^7$. Therefore, one sees that bremsstrahlung provides negligible energy loss to the collider as compared to pair production. Also, bremsstrahlung production of $e^+e^-$ pairs, being a higher order process (it is the decay of a "virtual" bremsstrahlung photon into an $e^+e^-$ pair), is negligible compared to direct pair production. This is essentially due to the large mass of the ions which causes only a very small acceleration of them by means of their Coulomb repulsion.

To conclude this section, we calculate in a similar way the energy loss of high-energy (heavy) ions of charge $Z_1$ passing through a medium of density $\rho$ and charge $Z_2$. This is relevant for the stopping power of cosmic rays. In this case, we can assume complete target screening. The energy loss per unit length due to $e^+e^-$ pair creation is found to be

$$\frac{dE}{dx} = -\frac{56}{9\pi} r_e^2 m_e \rho (Z_1 Z_2 \alpha)^2 \gamma \{\ln (183/Z^{1/3}) - \tfrac{1}{42} - \bar{f}(Z, Z_2)\}, \tag{3.15}$$

where $\rho$ is the number of target nuclei per unit volume, and $\bar{f}(Z_1, Z_2) = [Z_1 f(Z_1) + Z_2 f(Z_2)]/(Z_1 + Z_2)$ is a correction function which accounts for the elastic scattering of the electron and positron in the Coulomb field of both nuclei after they are created (see sect. 7.3 of ref. [3]). Being linear in $\gamma$, this mechanism will, for high enough energies, exceed the stopping power due to the atomic ionization, given by the Bethe-Bloch formula [18])

$$\left(\frac{dE}{dx}\right)_I = 4\pi r_e^2 m_e \rho Z_1^2 \{\ln |(2m_e \gamma^2/I) - 1\}, \tag{3.16}$$

where $I \simeq 16/Z_2^{1/3}$ eV.

In fig. 2 we show the ratio between stopping power, $dE_{pe}$, of cosmic rays by means of $e^+e^-$ production and the stopping power, $dE_I$, by means of atomic ionization for (naked) Fe nuclei penetrating several targets. One sees that for large

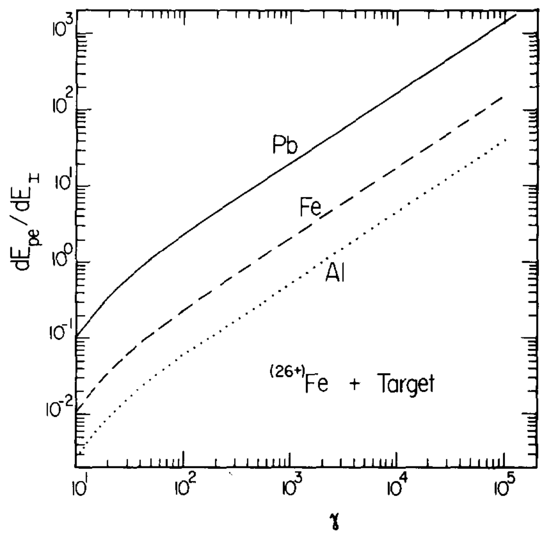


Fig. 2. The ratio $dE_{pe}/dE_I$ between the energy loss by pair production and that one arising from atomic ionization is shown as a function of $\gamma$, for various values of the charge $Z_2$ of the medium. As a projectile, we take a Fe nucleus ($Z_1 = 26$).

$\gamma$, $e^+e^-$ production is by far the dominant mechanism for the energy loss of heavy-ion cosmic rays.

## 4. $\gamma\gamma$ physics with relativistic heavy ions

The appropriate tool to study $\gamma\gamma$ physics is $e^+e^-$ colliders [19]. Essentially due to the enhancement factor of about $Z^4(\leq 10^8)$ in the $2\gamma$ cross section [20], interesting possibilities open up for peripheral ultra-relativistic heavy-ion colliders. Strong background problems will certainly have to be overcome in an experimental realization of such a programme. If one could selectively trigger on peripheral processes, where "the ions come in as they come out", the background may be strongly reduced.

It is the purpose of this section to illustrate the possibilities for $\gamma\gamma$ physics at ultra-relativistic heavy-ion colliders.

Recently, the invariant mass spectrum of lepton pairs produced in peripheral relativistic heavy-ion collisions was calculated by Alexander *et al.* [21]. Using the formulations of ref. [20] the cross section is given by

$$\frac{d\sigma}{dm_{\ell\ell}^2} = \left(\frac{4Z_1Z_2\alpha}{\pi}\right)\frac{1}{3m_{\ell\ell}^2}\left[\ln\left(\frac{2\gamma}{\sqrt{R_1R_2}m_{\ell\ell}}\right)\right]^3\sigma_{\gamma\gamma\to\ell^+\ell^-} \tag{4.1}$$

with $\hbar = c = 1$, and where $\sigma_{\gamma\gamma\to\ell^+\ell^-}$ is the cross section for lepton pair creation (see e.g. ref. [18]). The invariant mass of the lepton pair is denoted by $m_{\ell\ell}$. The length parameter $\sqrt{R_1R_2}$ denotes a minimum impact parameter cut-off. For $\ell = e$, due to the small mass of the electron, one should use the electron Compton wavelength $1/m_e$ for this parameter [14,20]. Indeed, as a function of the impact parameter $b$ in the collision the probability to create a $e^+e^-$ pair is approximately constant up to $b \simeq 1/m_e$. For larger values of $b$ the probability decreases as $1/b^2$ up to a maximum impact parameter of order of $\gamma/m_e$. Beyond this value, the probability decreases exponentially, this justifies the above approximation for $\gamma \gg 1$. Especially for low values of $\gamma$, this point needs further theoretical study. Inserting the $\sigma_{\gamma\gamma\to e^+e^-}$ cross section [18] in the above formula we get

$$\frac{d\sigma}{dm_{e^+e^-}^2} = \frac{2}{3\pi}(Z_1Z_2\alpha)^2\frac{r_e^2}{m_e^2}F(\gamma, y)\,, \tag{4.2}$$

where $F(\gamma, y)$ is a universal function given by

$$F(\gamma, y) = (1-y)(1-y^2)\left\{(3-y^4)\ln\left(\frac{1+y}{1-y}\right) + 2y(y^2-2)\right\}\ln^3(\gamma\sqrt{1-y}) \tag{4.3a}$$

with

$$y = 1 - \frac{4m_e^2}{m_{e^+e^-}^2}\,. \tag{4.3b}$$

In fig. 3a we show the invariant mass spectrum for $e^+e^-$ pair production, represented by the function $F$, for $\gamma = 100$ and $\gamma = 4000$ plotted against $m^2_{e^+e^-}/4m^2_e$. Quite similar to the more involved numerical studies of Alexander *et al.* [21]), we obtain a strong peak in the invariant mass spectrum at low energies (for $m^2_{e^+e^-} \simeq 8m^2_e$). That means that the created electron, or positron, will have on average a kinetic energy of about one half of its rest mass. This peak value rises only very slowly with the collider energy. It can be quite simply traced to the folding of the $\gamma\gamma \to e^+e^-$ cross section with the $\gamma\gamma$ luminosity (see eq. (4.1)).

In the case of $\mu^+\mu^-$ production the Compton wavelength is smaller than the nuclear radii, and one uses $\sqrt{R_1 R_2}$ as the lower cut-off parameter. The invariant

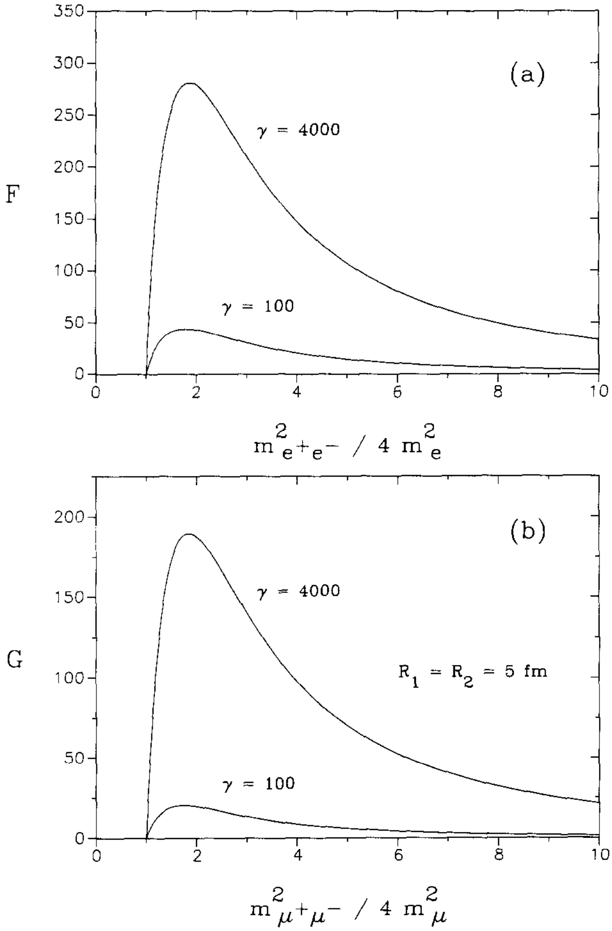


Fig. 3. (a) The dimensionless function $F(\gamma, y)$ as defined by eq. (4.3a) is shown as a function of $m^2_{e^+e^-}/4m^2_e = (1-y)^{-1}$. We take $\gamma = 100$ and $\gamma = 4000$, respectively. The differential cross section $d\sigma/dm^2_{e^+e^-}$ is obtained from eq. (4.2). (b) The dimensionless function $\tilde{G}(\gamma, y, \sqrt{R_1 R_2})$ is shown for $R_1 = R_2 = 5$ fm as a function of $m^2_{\mu^+\mu^-}/4m^2_\mu$. We take $\gamma = 100$ and $\gamma = 4000$, respectively.

mass spectrum is given by

$$\frac{d\sigma}{dm^2_{\mu^+\mu^-}} = \frac{2}{3\pi}(Z_1 Z_2 \alpha)^2 \frac{r^2_\mu}{m^2_\mu} G(\gamma, y, \sqrt{R_1 R_2}) , \tag{4.4a}$$

where

$$G(\gamma, y, \sqrt{R_1 R_2}) = \frac{F(\gamma, y)}{\ln^3(\gamma\sqrt{1-y})} \ln^3\left(\frac{\gamma}{m_\mu}\sqrt{\frac{1-y}{R_1 R_2}}\right) . \tag{4.4b}$$

In fig. 3b the adimensional function $G$ is displayed of a typical value of $R_1 = R_2 =$ 5 fm and for $\gamma = 100$ and 4000.

Again, the usual shape of the invariant mass spectra, which varies slowly (except for the increasing of the height of its peak with increasing $\gamma$) with $\gamma$ as found in ref. [21]), is reproduced.

In principle, the $Z^4$ factor in the cross section presents an enormous advantage of ultra-relativistic heavy-ion colliders for $\gamma\gamma$ physics as compared to $e^+e^-$ machines. We restrict ourselves here to presenting some typical numbers in order to illustrate the potential of the method. A real assessment, of course, will have to carefully consider possible detectors as well as the strong interaction background problem.

In ref. [20]) the $\gamma\gamma$ production of $C = +1$ mesons R was directly calculated in terms of their $\gamma\gamma$ partial widths $\Gamma(\mathrm{R} \to \gamma\gamma)$, of their mass $m_\mathrm{R}$ and spin $J_\mathrm{R}$. The cross section for their production in relativistic heavy-ion collision is

$$\sigma_c = \tfrac{128}{3}(Z_1 Z_2 \alpha)^2 \frac{\Gamma(\mathrm{R} \to \gamma\gamma)}{m^3_\mathrm{R}} (2J_\mathrm{R} + 1) \ln^3\left(\frac{2\gamma}{m_\mathrm{R}\sqrt{R_1 R_2}}\right) . \tag{4.5}$$

In table 2 we collect the results for some relevant examples, in a collision at RHIC with $Z = 92$ and $\gamma = 100$, and at LHC with $Z = 82$ and $\gamma = 4000$. We use $R_i = 1.2\, A_i^{1/3}$ fm.

The mass of the $\eta_b$ is taken from the theoretical quark model calculations [22]). Note that the mass of $\eta_b$ is very high and the approximation (4.5) does not apply for the RHIC energy. In this case one should use the exponential tail of the equivalent photon spectrum for a better evaluation [3]).

TABLE 2

Cross sections for the production of $C = +1$ mesons at RHIC (with $Z = 92$) and at LHC, with $Z = 82$

| Meson R | Mass (MeV) | $\Gamma$ (R $\to \gamma\gamma$) | RHIC $Z = 92$, $\gamma = 100$ | LHC $Z = 82$, $\gamma = 4000$ |
|---|---|---|---|---|
| $\pi^0$ | 135 | 9 eV | 12.7 mb | 62 mb |
| $\eta$ | 549 | 1 keV | 5.3 mb | 55 mb |
| $\eta'$ | 958 | 5 keV | 2.3 mb | 39 mb |
| $\eta_c$ | 2981 | 6.3 keV | 5.4 μb | 0.8 mb |
| $\eta_b$ | 9366 | 0.41 keV | - | 0.9 μb |

In this context, the suggestion of Papageorgiu [23]) and Grabiak *et al.* [24]) of producing neutral Higgs particles is especially interesting (see also ref. [25])). The partial width $\Gamma(\mathrm{H}^0 \to \gamma\gamma)$ as taken from the standard electro-weak model is [26])

$$\Gamma_{\mathrm{H}\to\gamma\gamma} = \frac{\alpha^2}{8\sqrt{2}\pi^3} G_{\mathrm{F}} m_{\mathrm{H}}^3 |I|^2 , \tag{4.6}$$

where $G_{\mathrm{F}}$ is the Fermi constant and $m_{\mathrm{H}}$ is the Higgs mass. $I$ is a factor containing contributions from intermediate lepton, quark and gauge boson loops, and is of order one (see. e.g. ref. [23])). Then, the cross section for Higgs boson production by means of the two-photon mechanism in RHI collisions has the form

$$\sigma_{\mathrm{c}} = \frac{16}{3\sqrt{2}\pi^3} (Z_1 Z_2 \alpha^2)^2 G_{\mathrm{F}} |I|^2 \ln^3 \left( \frac{2\gamma}{m_{\mathrm{H}} \sqrt{R_1 R_2}} \right) . \tag{4.7}$$

For the LHC, in $^{208}\mathrm{Pb} + {}^{208}\mathrm{Pb}$ collisions, and using a Higgs mass of 50 GeV and taking $I \sim 1$, we find a cross section of about 0.23 nb. The two-gluon mechanism $\mathrm{gg} \to \mathrm{H}^0$ has about the same cross section in proton collisions at 40 TeV c.m. energy, but is accompanied with a myriad of other particles which are produced in hadronic scattering. In RHI colliders, on the other hand, a suitable choice of experimental set-ups, selecting low-multiplicity events and small transverse momenta, maybe a more favourable method to detect the Higgs boson.

The advantage over pp colliders (like SSC) may be especially true for rather low values of the Higgs boson mass. This is due to the rapid decrease of the $\gamma\gamma$ luminosity with increasing invariant mass.

Even the investigation of continuum final states could be envisaged. Using the equivalent photon method, it is also quite straightforward to obtain differential cross sections, as shown above in the Higgs boson example.

Another interesting process which could be studied is $\gamma + \gamma \to \gamma + \gamma$, the elastic scattering of light on light (see e.g. ref. [18])). Its cross section involves an additional factor of $\alpha^2$ as compared to the pair production, it is, therefore, rather small and it has never been possible to study it directly. On the other hand, the elastic scattering of $\gamma$'s in the Coulomb field of nuclei has been experimentally investigated (Delbrück scattering). It is also a good possibility to study elastic scattering of two photons with RHI collisions by means of the process $Z_1 + Z_2 \to Z_1 + Z_2 + \gamma + \gamma$. In ref. [20]) it was shown that the total cross section for this process in RHI collisions is entirely dominated by high-energy photons with $\omega \gg m_{\mathrm{e}}$. The cross section was found to be [20]) (correcting a printing error in that reference)

$$\sigma_{Z_1 Z_2 \to Z_1 Z_2 \gamma\gamma} = 2.54 (Z_1 Z_2 \alpha^2)^2 r_{\mathrm{e}}^2 [\ln^3 \xi - \tfrac{3}{2} \ln^2 \xi + \tfrac{3}{2} \ln \xi - \tfrac{3}{4}] , \tag{4.8}$$

where $\xi = \gamma / m_{\mathrm{e}} \sqrt{R_1 R_2}$. For the LHC with U+U beams, one finds a cross section of 51 b. This rather large effect (although orders of magnitude smaller than the $\mathrm{e}^+\mathrm{e}^-$ production) might be used as an alternative to the experimental study of $\gamma\gamma$ elastic scattering, or may be viewed as an unwanted "background". In summary, due to the suppression of the bremsstrahlung mechanism, as compared to the $e^+e^-$ collisions, the heavy ions may be an advantage to study $\gamma\gamma$ processes, however, background problems are certainly severe and must be studied more carefully in the future.

## 5. Conclusion

It has become clear in the course of this investigation, that electromagnetic effects in peripheral collisions at RHI colliders are a serious beam loss mechanism, as well as a potential tool for new physics. The main loss mechanisms are giant dipole resonance excitations and pair production with atomically bound electrons. Our calculations involve rather well established concepts in QED and nuclear physics, and therefore our predictions can be considered as safe. Especially at LHC conditions, the contributions of the extremely hard component of the equivalent photon spectrum can only be estimated at present. They are expected to be sizeable, although not larger than giant dipole resonance contributions. On the other hand, such collisions could be used to investigate $\gamma$-nucleus cross sections in the energy range up to several 100 TeV.

Especially striking is the production of $e^+e^-$ pairs (to a lesser extent also $\mu^+\mu^-$ and $\tau^+\tau^-$ pairs). Is this unwanted, or could these particles be useful for some other purpose? (cf. the somehow analogous situation of synchrotron radiation in electron rings).

The possibility to use RHI collisions for $\gamma\gamma$ physics has to be studied more carefully in the future. Apart from theoretical predictions it will be necessary to investigate the needs for detectors specific to the low multiplicity in these peripheral collisions, as well as the influence of the strong background from the central nucleon collisions.

One of the authors (G.B.) is very grateful to Drs. D. Brandt and A. Sandoval for very illuminating discussions on relativistic heavy-ion colliders, as well as for their encouragement.

## References

1) "Conceptual design of the relativistic heavy ion collider (RHIC)", Brookhaven National Laboratory, Report BNL 51932 (May, 1986)
2) D. Brandt, LHC/Note No. 87, and private communication; see also Physics Today, March 1988, p. 17
3) C.A. Bertulani and G. Baur, Phys. Reports **163** (1988) 299
4) G. Baur and C.A. Bertulani, Nucl. Phys. **A482** (1988) 313c
5) G. Baur and C.A. Bertulani, contribution to the 3rd. Int. Conf. on nucleus-nucleus collisions, St. Malo 1988, p. 234
6) J.C. Hill, F.K. Wohn, J.A. Winger and A.R. Smith, Phys. Rev. Lett. **60** (1988) 999
7) C. Brechtmann and W. Heinrich, Z. Phys. **A330** (1988) 407

8) G. Baur and C.A. Bertulani, Phys. Lett. **B174** (1986) 23; Phys. Rev. **C34** (1986) 1654;
P. Braun-Munzinger *et al.*, Proposal 814 submitted to the AGS program committee, SUNY at Stony Brook, accepted 1985 (unpublished)
9) G. Baur, Z. Phys. **A332** (1989) 203;
G. Baur and N. Baron, J. of Phys. **G15** (1989) 661;
H. Emling, Proc. 8th high energy heavy ion study, Berkeley, November 16–20, 1987, ed. J.W. Harris and G.J. Wozniak p. 503
10) T.H. Bauer, R.D. Spital, D.R. Yennie and F.M. Pipkin, Rev. Mod. Phys. **50** (1978) 261
11) C. Brechtmann and W. Heinrich, Z. Phys. **A331** (1988) 463;
P.B. Price, R. Guaxiao and W.T. Williams, Phys. Rev. Lett. **61** (1988) 2193
12) D.O. Caldwell *et al.*, Phys. Rev. Lett. **40** (1978) 1222
13) G. Baur and C.A. Bertulani, Phys. Rev. **C35** (1987) 836
14) C.A. Bertulani and G. Baur, Revista Brasileira de Fisica **18** (1988) 525, 539
15) V.M. Budnev *et al.*, Phys. Reports **15** (1974) 182
16) L.D. Landau and E.M. Lifshitz, Phys. Zs. Sowjet **6** (1934) 244
17) U. Becker N. Grün and W. Scheid, J. of Phys. **B20** (1987) 2075
18) A.I. Akhiezer and V.B. Berestetiskii, Quantum electrodynamics (Interscience, New York, 1965);
L.D. Landau and E.M. Lifshitz, Lehrbuch der Theoretischen Physik, vol. IV (Academie, Berlin 1980)
19) P.M. Zerwas, Invited talk presented at the photon-photon workshop, Jerusalem, April 1988;
H. Kolanoski and P.M. Zerwas, Two-photon physics in high-energy electron–positron physics, ed. A. Ali and P. Söding (World Scientific, Singapore, 1988)
20) G. Baur and C.A. Bertulani, Z. Phys. **A330** (1988) 77
21) G. Alexander, E. Gotsman and U. Maor, Z. Phys. **C34** (1987) 329
22) E. Eichten and F. Feinberg, Phys. Rev. **D23** (1981) 2724
23) E. Papageorgiu, Phys. Rev. **D40** (1989) 92
24) M. Grabiak, B. Müller, W. Greiner, G. Soff and P. Koch, J. of Phys. **G15** (1989) L25;
G. Soff, J. Rau, M. Grabiak, B. Müller and W. Greiner, GSI-89-55 preprint (June 1989)
25) M. Drees, J. Ellis and D. Zeppenfeld, Phys. Lett. **B223** (1989) 454
26) J. Ellis, M.K. Gailland and D.V. Nanopoulos, Nucl. Phys. **B106** (1976) 292;
R. Bates and J.N. Ngo, Phys. Rev. **D33** (1985) 657;
L.B. Okun, Leptons and quarks (North-Holland, Amsterdam, 1982)